PNAS RESEARCH ARTICLE | MICROBIOLOGY OPEN ACCESS

Omicron mutations enhance infectivity and reduce antibody neutralization of SARS-CoV-2 virus-like particles

Abdullah M. Syed[a,b], Alison Ciling[a,b], Taha Y. Taha[a], Irene P. Chen[a,f], Mir M. Khalid[a], Bharath Sreekumar[a], Pei-Yi Chen[a,c], G. Renuka Kumar[a], Rahul Suryawanshi[a], Ines Silva[d], Bilal Milbes[d], Noah Kojima[e], Victoria Hess[d], Maria Shacreaw[d], Lauren Lopez[d], Matthew Brobeck[d], Fred Turner[d], Lee Spraggon[d], Takako Tabata[a], Melanie Ott[a,f,g,1], and Jennifer A. Doudna[a,b,h,i,j,k,l,1]

Edited by Peter Sarnow, Stanford University School of Medicine, Stanford, CA; received January 12, 2022; accepted June 5, 2022

The severe acute respiratory syndrome coronavirus 2 (SARS-CoV-2) Omicron variant contains extensive sequence changes relative to the earlier-arising B.1, B.1.1, and Delta SARS-CoV-2 variants that have unknown effects on viral infectivity and response to existing vaccines. Using SARS-CoV-2 virus-like particles (VLPs), we examined mutations in all four structural proteins and found that Omicron and Delta showed 4.6-fold higher luciferase delivery overall relative to the ancestral B.1 lineage, a property conferred mostly by enhancements in the S and N proteins, while mutations in M and E were mostly detrimental to assembly. Thirty-eight antisera samples from individuals vaccinated with Pfizer/BioNTech, Moderna, or Johnson & Johnson vaccines and convalescent sera from unvaccinated COVID-19 survivors had 15-fold lower efficacy to prevent cell transduction by VLPs containing the Omicron mutations relative to the ancestral B.1 spike protein. A third dose of Pfizer vaccine elicited substantially higher neutralization titers against Omicron, resulting in detectable neutralizing antibodies in eight out of eight subjects compared to one out of eight preboosting. Furthermore, the monoclonal antibody therapeutics casirivimab and imdevimab had robust neutralization activity against B.1 and Delta VLPs but no detectable neutralization of Omicron VLPs, while newly authorized bebtelovimab maintained robust neutralization across variants. Our results suggest that Omicron has similar assembly efficiency and cell entry compared to Delta and that its rapid spread is due mostly to reduced neutralization in sera from previously vaccinated subjects. In addition, most currently available monoclonal antibodies will not be useful in treating Omicron-infected patients with the exception of bebtelovimab.

Omicron | SARS-CoV-2 | virus-like particles

Significance

Severe acute respiratory syndrome coronavirus 2 (SARS-CoV-2) Omicron contains extensive mutations and demonstrates enhanced transmission. We used virus-like particles to examine the assembly and neutralization of Omicron and found that Omicron and Delta showed ~4.6-fold higher assembly and cell entry relative to the ancestral lineage. S and N protein mutations improved assembly and entry while E mutations inhibited assembly. Omicron also escapes neutralization from antisera of vaccinated or convalescent individuals by ~15-fold. Boosting increased neutralization titers against Omicron and restored neutralization in all subjects compared to one out of eight before boosting. Our results suggest that the rapid spread of Omicron is due to more efficient assembly, cell entry, and escape from antibody neutralization from existing vaccines or previous infection

Understanding the molecular determinants of severe acute respiratory syndrome coronavirus 2 (SARS-CoV-2) viral fitness is central to effective vaccine and therapeutic development. The emergence of viral variants including Delta and Omicron underscores the need to assess both infectivity and antibody neutralization, but biosafety level 3 handling requirements slow the pace of research on intact SARS-CoV-2. Although vesicular stomatitis virus and lentivirus pseudotyped with the SARS-CoV-2 spike (S) protein enable evaluation of S-mediated cell binding and entry via the ACE2 and TMPRSS2 receptors, they cannot determine effects of mutations outside the S gene (1, 2). To address these challenges, we developed SARS-CoV-2 virus-like particles (SC2-VLPs) comprising the S, N, M, and E structural proteins and a packaging signal-containing messenger RNA (mRNA) that together form RNA-loaded capsids capable of spike-dependent cell transduction (3). This system faithfully reflects the impact of mutations in structural proteins that are observed in infections with virus isolates, enabling rapid testing of SARS-CoV-2 structural gene variants for their impact on both infection efficiency and antibody or antiserum neutralization.

Results

Using the SC2-VLP system, we first generated a set of plasmid constructs encoding the S, N, M, and E structural proteins derived from the B.1, B.1.1, Delta, and Omicron SARS-CoV-2 viral variants (*SI Appendix*, Table S1). We generated SC2-VLPs by cotransfecting packaging cells (293T cells) with three plasmids encoding these structural proteins and a fourth plasmid encoding luciferase mRNA linked to a SARS-CoV-2 packaging signal (3). Particles secreted from these packaging cells were filtered and incubated with receiver 293T cells stably coexpressing ACE2 and TMPRSS2 (Fig. 1*A*). To compare the effects of the different structural gene variants on infectivity, we used the structural genes from SARS-CoV-2 B.1 as the point of reference from which to

This article is a PNAS Direct Submission.

[1]To whom correspondence may be addressed. Email: melanie.ott@gladstone.ucsf.edu or doudna@berkeley.edu.

This article contains supporting information online at http://www.pnas.org/lookup/suppl/doi:10.1073/pnas.2200592119/-/DCSupplemental.

Published July 19, 2022.

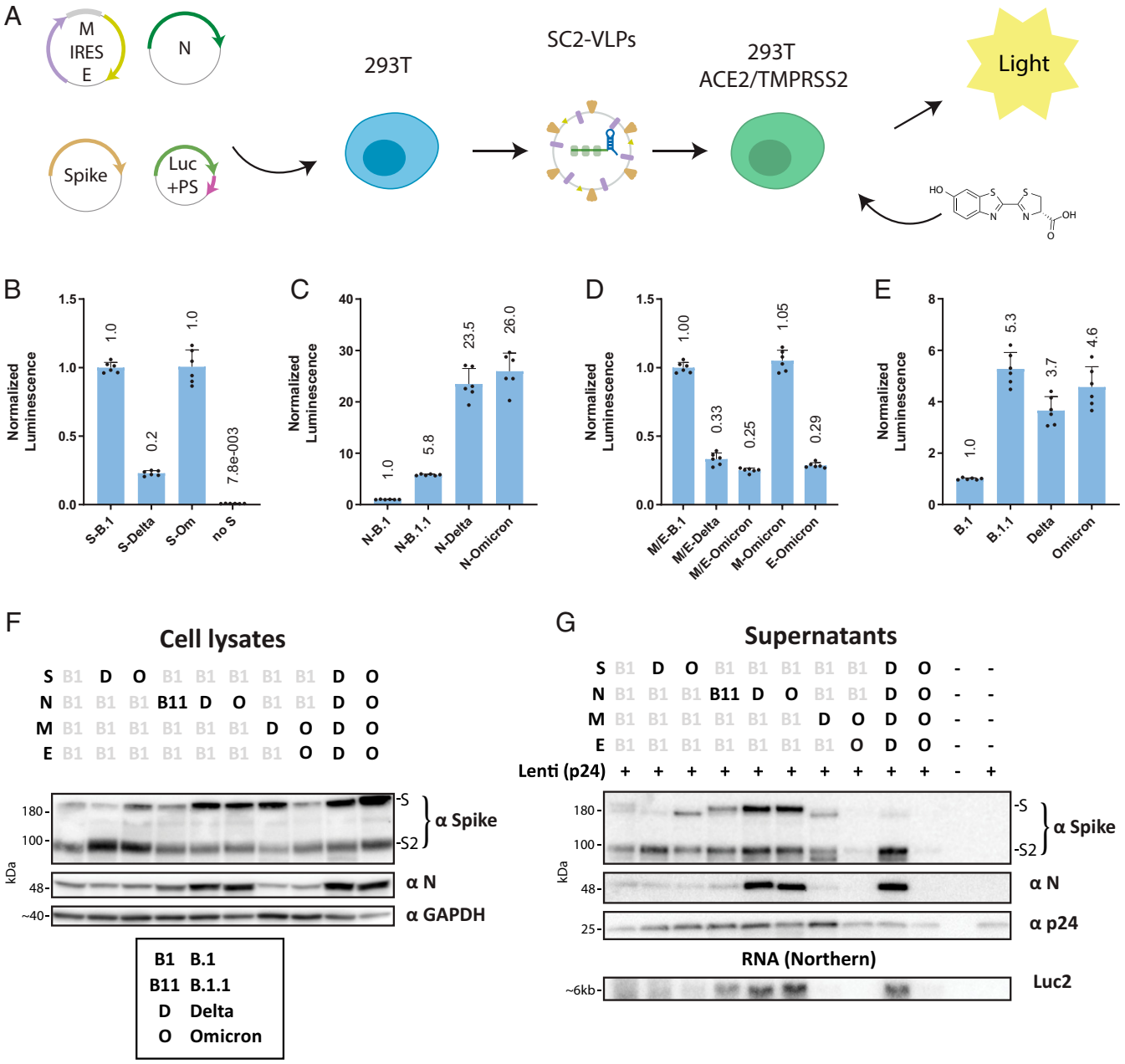

Fig. 1. Omicron structural gene variants alter infectivity of SC2-VLPs. (*A*) Sequence differences in genes encoding the structural proteins S, E, M, and N between B.1, B.1.1, Delta, and Omicron viral variants (vertical lines); Omicron-Class 1 and Omicron-Class 3 mutations were created for this study. (*B*) Workflow for generating SC2-VLPs and testing their ability to transduce ACE2- and TMPRSS2-expressing 293T cells; SC2-VLPs assembled in packaging cells transformed with plasmids encoding S, E, M, and N genes as well as a luciferase mRNA fused to the SARS-CoV-2 packaging signal are tested for receptor-mediated cell transduction using a luciferase detection assay. (*C*–*E*) Luminescence measured as a function of VLPs generated with the component protein shown, in a background of B.1 genes (see text for details). (*F*) Western blot of cell lysates from cells transfected to generate VLPs stained for N, S, and GAPDH as a loading control. (*G*) Western and Northern blots of particles purified from supernatants by 20% sucrose cushion ultracentrifugation. Staining for N, S, and p24 in the Western blots. Note: lentivirus was added to all supernatants as a loading control for purification. Luc2 mRNA was stained for with a ^{32}P-labeled probe targeting the luciferase gene. Quantification and statistical comparison of blots in *F* and *G* are shown in *SI Appendix*, Fig. S1.

vary each structural gene individually since it is ancestral to all currently circulating variants. For each combination of structural proteins, we evaluated the luciferase expression in receiver cells, the expression level of the S and N proteins in packaging cells, and abundance of the S and N proteins and luciferase RNA in the supernatant (Fig. 1 *B*–*G*).

We first examined the S genes of B.1, Delta, and Omicron variants using VLPs that otherwise contained B.1 gene versions. We found that relative to S-B.1 (identical to S-B.1.1) the Delta S-variant produced VLPs that were only 40% as infectious (Fig. 1*B*). In contrast, the Omicron S gene in the context of the B.1 background generated higher VLP infectivity compared to ancestral S-B.1 (Fig. 1*B*). Expression of S in packaging cells and supernatant (Fig. 1 *F* and *G* and *SI Appendix*, Fig. S1) was similar between these variants, suggesting that this discrepancy is due to intrinsic efficiency of the Omicron S protein when incorporated into VLPs. Interestingly, pseudotyped lentiviral particles show the opposite pattern of increased entry for S-Delta and reduced entry for S-Omicron (*SI Appendix*, Fig. S2). In addition, the cleavage and processing of S also varied not only between different S-variants but also when coexpressed with different M and N variants (Fig. 1 *F* and *G*). These results

suggest that viral genetic context including proteolytic processing and secretion pathway influences S gene effects on the ability of viral particles to transduce cells, and also that some S gene mutations such as those in Omicron may dominate cell infectivity outcomes.

We next compared the effects of N variants on infectivity of VLPs generated using B.1 genes. The N gene was found previously to have a pronounced influence on infectivity and RNA packaging efficiency (3). Required for replication, RNA binding, packaging, stabilization, and release, the N protein includes a seven-amino-acid mutational hotspot (N:199 to 205) in a region linking the N- and C-terminal domains. Notably, B.1.1, Delta, and Omicron, but not B.1, include mutations at R203 that were found previously to enhance VLP infectivity and RNA packaging (*SI Appendix*, Table S2) (3). The N-Delta and N-Omicron variants generated significantly higher N expression in the supernatant with higher RNA packaging (Fig. 1*G* and *SI Appendix*, Fig. S1) and infectivity that was enhanced relative to both B.1 and B.1.1 variants, consistent with the N protein's playing a central role in viral packaging and cell transduction efficiency (Fig. 1*C*).

Omicron contains three mutations in the M protein and one mutation in the E protein relative to B.1/Delta. VLPs generated using either M or E protein from Omicron, but with B.1 versions of the other structural components, showed levels of infectivity that were reduced relative to those measured for the B.1 VLPs (Fig. 1*D* and *SI Appendix*, Tables S3 and S4). In particular, these mutations reduce the assembly of VLPs as seen by the reduced intensity of N and S in the supernatant (Fig. 1 *F* and *G*). This finding suggests that some Omicron mutations reduce particle assembly and may reduce viral fitness. To test if these effects are mitigated by mutations in other structural proteins, we also tested VLPs generated using the combined structural protein mutations for each variant. We found that Omicron VLPs were overall 4.6 times as infectious as VLPs generated using B.1 structural proteins but similar in infectivity to VLPs generated using Delta or B.1.1 structural proteins, consistent with observed enhancements (S and N) and deficits (M and E) seen in the individual proteins (Fig. 1*E*).

We next tested the VLP neutralization capability of antisera collected from 38 individuals 4 to 6 wk postvaccination with Pfizer/BioNTech, Moderna, or Johnson & Johnson vaccines, or convalescent sera from unvaccinated COVID-19 survivors. The antisera were collected from participants aged 18 to 50 y enrolled in a clinical trial led by Curative, and SARS-CoV-2 immunoglobulin G (IgG) antibodies were quantified with an enzyme-linked immunosorbent assay (ELISA) (*SI Appendix*, Table S5). The serum was heat-inactivated at 56 °C for 30 min and then incubated with VLPs at dilutions 1/20, 1/80, 1/320, 1/1280, 1/5120, and 1/20,480 for a total of six dilutions. VLPs were generated with B.1 structural genes except for N-R203M, which we previously found to enhance assembly and increase the dynamic range of our neutralization assay. In initial experiments using B.1 spike we found that sera from both Pfizer/BioNTech- and Moderna-vaccinated individuals yielded high neutralization titers with medians of 549 and 490, respectively (Table 1). Sera from Johnson & Johnson–vaccinated and convalescent patients had lower titers with median of 25 and 35, respectively (Table 1), matching the low levels of SARS-CoV-2 IgG antibodies detected in this cohort (*SI Appendix*, Table S5). We also checked whether neutralizing titers as measured by VLPs correlated with titers measured using virus isolates or S-protein IgG measured by ELISA. We found that titers measured using VLPs correlated well with neutralization of virus isolates with $r^2 = 0.98$ but did not correlate with anti-S IgG, suggesting that some subjects may generate antibodies that bind but do not neutralize SARS-CoV-2 (*SI Appendix*, Figs. S3 and S4).

Table 1. Neutralization titers of vaccinated or convalescent individuals against S-variants

	B.1	Delta	Omicron	OmC1	OmC3
PF0002	5900	880	768	4006	2435
PF0004	4396	1248	204	1206	1244
PF0005	549	185	20	172	130
PF0006	194	52	17	34	68
PF0007	752	319	30	190	357
PF0009	1159	204	178	483	475
PF0011	824	241	43	166	289
PF0012	282	108	19	57	140
PF0013	152	110	18	45	85
PF0016	37	1	17	9	31
PF0017	295	118	37	110	151
M0002	3830	727	692	3185	1771
M0003	375	75	26	102	173
M0004	25608	6105	3524	15008	10995
M0005	376	130	54	133	174
M0006	450	80	24	229	178
M0007	531	131	41	205	215
M0008	186	76	17	94	111
M0009	608	168	41	205	245
M0010	171	35	2	47	60
M0011	823	158	53	238	232
JJ0002	60	2	16	16	11
JJ0003	58	10	15	6	13
JJ0005	26	7	19	35	15
JJ0006	26	9	16	10	13
JJ0007	11	12	14	7	18
JJ0008	25	16	55	14	19
JJ0009	10	8	14	0	14
JJ0010	15	7	20	6	7
JJ0011	20	5	12	3	12
PC0002	51	44	43	19	12
PC0003	7	22	20	9	25
PC0006	5	0	15	5	5
PC0007	31	0	24	12	24
PC0008	39	323	27	14	26
PC0009	268	113	24	104	14
PC0011	432	19044	77	44	291
PC0013	0	112	8	0	30
Naïve	5	11	19	9	2

Numbers indicate dilution factors that yield 50% neutralization. Higher numbers indicate better neutralization. Red fill indicates undetectable neutralization at the lowest (1/20) dilution.

We then substituted the S-gene with S-variants previously tested, as they have varying mutations in the receptor binding domain (RBD) known to affect neutralization. We tested the neutralization capacity of each patient's serum against VLPs representing S from B.1, Delta, or Omicron viral variants (Fig. 2 *A–D*). There was a pronounced decrease of 15- to 18-fold in potency against Omicron, with intermediate effects on Delta, for the antisera from mRNA vaccine recipients (Fig. 2 *A–D* and Table 1). Limited efficacy was detected for any of the sera from those vaccinated with the adenovirus-based Johnson & Johnson vaccine and variable neutralization was observed for COVID-19 survivors (Table 1). We next examined whether Class 1 or Class 3 mutations were responsible for reduced neutralization in patient anti sera. For both S-OmC1 and OmC3 cases we found intermediate neutralization, suggesting that neutralization escape from patient sera is a function of several mutations acting in concert (*SI Appendix*, Fig. S5 *A–D*). Third-dose vaccination with the Pfizer vaccine increased titers against all variants including Omicron (Fig. 2 *E–H*, *SI Appendix*, Fig. S5 *E–G*, and Table 2) as measured at 16 and 21 d after the third dose. All eight sera from this cohort had low (median 64) neutralization titers against Omicron 21 d after their third dose, while only one out of eight had detectable neutralization prior to boosting (Fig. 2*G*). However, even after boosting we observed eightfold reduced neutralizing titers against Omicron compared to B.1, suggesting that Omicron is still able to partially escape neutralizing antibodies induced by vaccination with the ancestral S-B.1 (Fig. 2*H* and Table 2).

We next tested whether therapeutic and commercially available monoclonal antibodies could neutralize VLP entry mediated by the ancestral SARS-CoV-2 S protein or the S protein from Omicron. Therapeutic antibodies casirivimab (Regeneron),

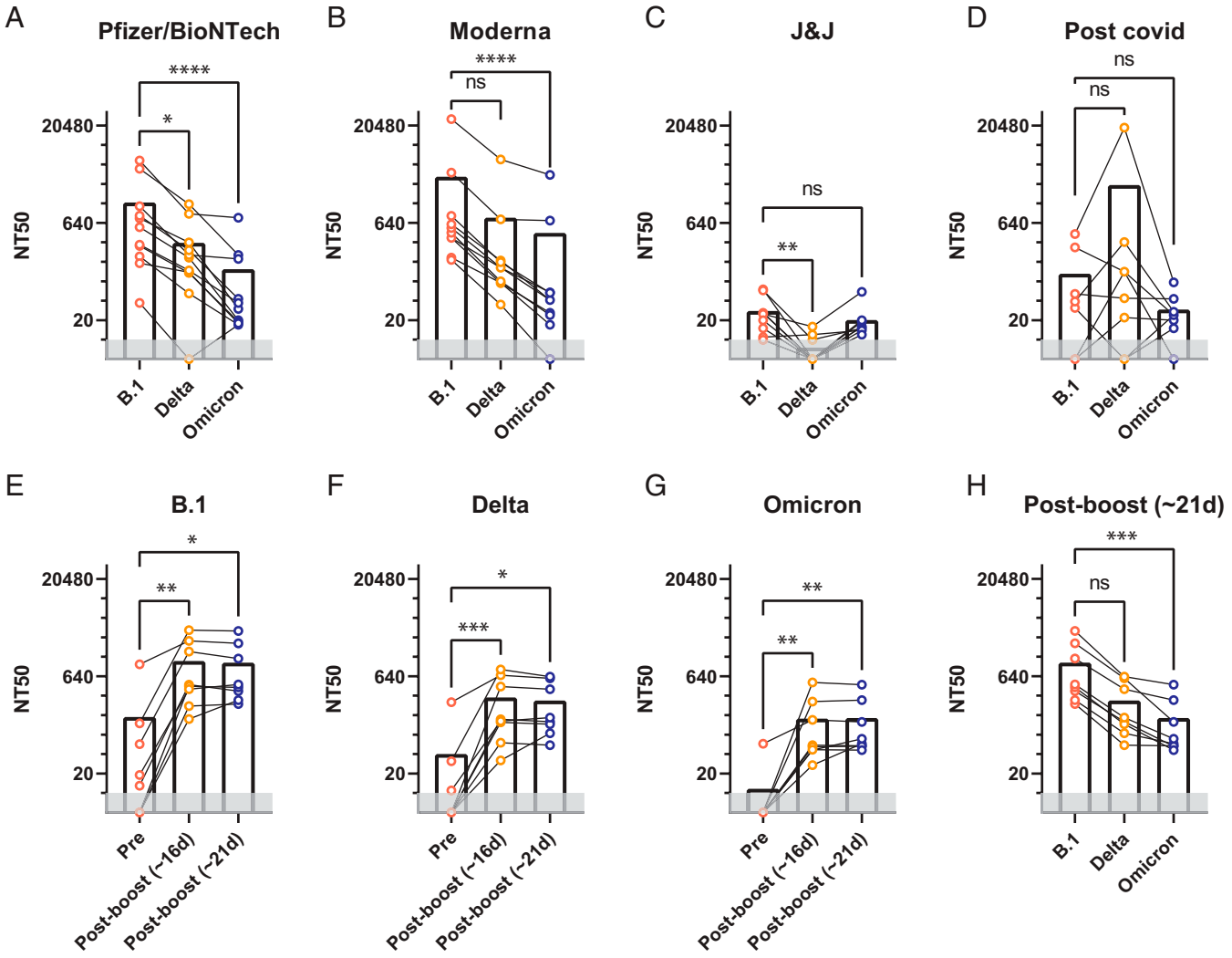

Fig. 2. Antiserum neutralization of VLPs generated with different S genes. (*A–D*) Fifty percent neutralization titers of sera isolated from individuals vaccinated using Pfizer/BioNTech, Moderna, and Johnson & Johnson vaccines or from convalescent COVID-19 patients. Neutralization curves were determined using VLPs with either S-B.1, S-Delta, or S-Omicron. (*E–H*) Neutralization titers of sera collected before and after third dose vaccination from individuals receiving the Pfizer/BioNTech vaccine. *$P < 0.05$, **$P < 0.01$, ***$P < 0.001$, ****$P < 0.0001$ evaluated using Friedman's exact test for repeated measures. ns, not statistically significant.

imdevimab (Regeneron), sotrovimab (Vir/GSK), and bebtelovimab (AbCellera/Eli Lilly) all demonstrated excellent neutralizing IC_{50}s (concentrations that inhibit response by 50%) against B.1 S protein, but only sotrovimab and bebtelovimab neutralized Omicron S protein (Fig. 3). Interestingly, sotrovimab was less effective against Delta and Omicron compared to B.1, while the recently authorized bebtelovimab had potent neutralization against all variants with an IC_{50} of less than 10 ng/mL.

We also generated S-variants containing Omicron mutations outside the RBD but containing only mutations within the RBD previously shown to inhibit binding by Class 1 (417N, 496S, 498R, 501Y) or Class 3 (440K, 446S, 496S, 498R) antibodies (*SI Appendix*, Table S1) (4). Previous studies have shown that the binding of casirivimab and imdevimab and other Class 1 and Class 3 antibodies is particularly sensitive to mutations at these residues. We generated VLPs using OmC1 or OmC3 S genes and evaluated the neutralization of casirivimab and imdevimab monoclonal antibodies (Table 3). Strikingly, although both antibodies had robust neutralization activity against B.1.1 or Delta VLPs, no activity was detected for either one against Omicron VLPs. We found that casirivimab was able to neutralize OmC3 but not OmC1, and imdevimab was able to neutralize OmC1 but not OmC3. This suggests that the six mutations within the Omicron RBD (K417N, N440K, G446S, G496S, Q498R, N501Y) are largely responsible for the failure of these monoclonal antibodies to neutralize Omicron S.

Table 2. Neutralization titers against S-variants of individuals vaccinated with two or three doses of the Pfizer vaccine

NT50 against S-B.1			NT50 against S-Delta			NT50 against S-Omicron			Time Lapsed between samples		
Pre boost	T1	T2	Pre boost	T1t	T2	Pre boost	T1	T2	T0 (Third dose-Second Dose) days	T1 (Days post booster shot)	T2 (Days post booster shot)
9	222	238	2	60	55	0	55	54	239	14	20
977	2251	2070	254	664	593	58	135	126	194	17	21
120	3311	3213	31	816	631	5	512	474	215	17	20
0	139	274	0	32	84	1	27	58	197	19	22
13	473	378	0	138	127	2	52	53	190	16	21
3	448	432	0	124	116	0	47	46	212	17	20
57	1537	1197	6	444	404	3	260	274	200	17	20
19	404	477	11	130	147	0	46	69	239	17	22

Each row represents one subject. Numbers indicate dilution factors that yield 50% neutralization. Higher numbers indicate better neutralization. Red fill indicates undetectable neutralization at the lowest (1/20) dilution. Last three columns indicate the time elapsed between doses for each individual.

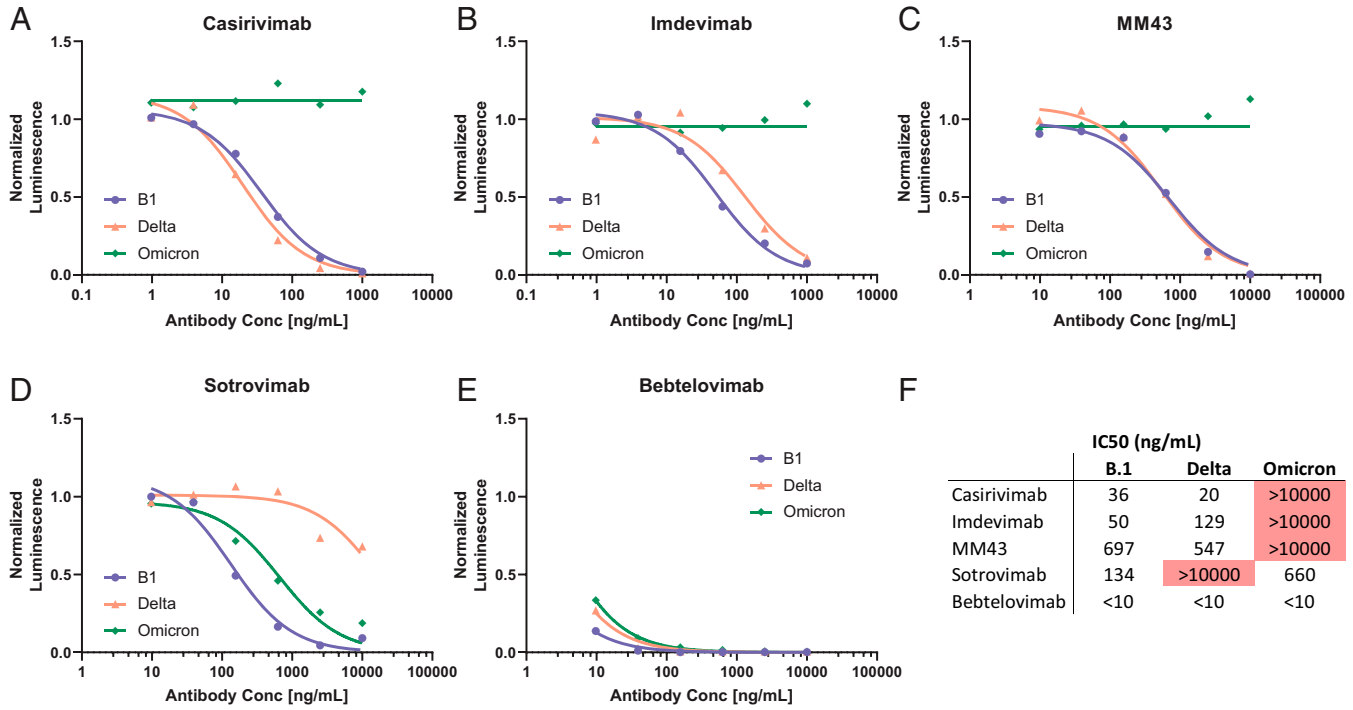

F

IC50 (ng/mL)	B.1	Delta	Omicron
Casirivimab	36	20	>10000
Imdevimab	50	129	>10000
MM43	697	547	>10000
Sotrovimab	134	>10000	660
Bebtelovimab	<10	<10	<10

Fig. 3. Monoclonal antibody neutralization of VLPs generated with different S genes. Neutralization curves and IC_{50} values of (A) casirivimab, (B) imdevimab, (C) MM43, (D) Sotrovimab, (E) Bebtelovimab against the S-variants: S-B.1, S-Delta, S-Omicron. (*F*) IC_{50} values for each monoclonal antibody.

Discussion

In summary, SARS-CoV-2 VLPs that transduce reporter mRNA into ACE2- and TMPRSS2-expressing cells enabled a rapid and comprehensive comparison of structural protein (S, E, M, N) variant effects on both particle infectivity and antibody neutralization. Using this system, we found that the Omicron versions of both S and N enhance VLP infectivity relative to ancestral viral variants including Delta. Omicron maintains mutations in the N mutational hotspot that were shown previously to confer markedly enhanced VLP infectivity (3). Surprisingly, Omicron M and E gene variants appear to compromise infectivity, at least in the context of ancestral versions of the other structural genes, implying that genes including S and N override less-fit versions of M, E, and perhaps other genes in the intact virus. Monitoring S and N gene evolution and determining why the N gene has such a pronounced effect on viral particle infectivity may enable development of better diagnostics, more broadly neutralizing vaccine development, and potentially new therapeutics.

Notably, all antisera from vaccinated individuals or convalescent sera from COVID-19 survivors showed reduced neutralization of Omicron VLPs relative to ancestral variants including Delta, with mRNA vaccines far surpassing a viral vector vaccine or natural infection in initial potency. These data do not account for T cell-based immunity induced by vaccination or prior infection. We also found that Omicron S mutations interfere with Class 1 and Class 3 monoclonal antibody binding, rendering some commercially available therapeutic antibodies completely ineffective. These results suggest that prior to vaccine boosting, antibodies produced by mRNA vaccines have 15- to 18-fold reduced efficacy against Omicron, and that the Johnson & Johnson vaccine produces limited neutralizing antibodies against any SARS-CoV-2 variant. Booster shots increase neutralization titers against Omicron but the titers remain much lower than for previous variants. Consistent with data from recent pseudovirus neutralization studies (5, 6), these findings support the use of mRNA vaccine boosters to enhance antibody-based protection against Omicron infection, in lieu of vaccines tailored to Omicron itself.

Our approach for analyzing the impact of mutations in structural proteins has a few limitations. We assume that mutations in the structural proteins act independently of each other and of the other nonstructural genes of the virus. Our results are consistent with additive effects of N, M, E, and S mutations, but this may not be the case when combined with other viral proteins. It would be interesting to see if similar results would be obtained in infectious clones incorporating the entire genome and testing these mutations combinatorially, but this is infeasible due to the large number of mutations. In addition, we cannot separate infectious VLPs from defective particles and exosomes, which may affect the interpretations of our conclusions regarding the compositions of VLPs.

Table 3. IC_{50} of casirivimab and imdevimab against S-variants (nanograms per milliliter)

	Casirivimab	Imdevimab
B.1	36	34
Delta	21	125
Omicron	>1000	>1000
OmC1	>1000	39
OmC3	56	>1000

Smaller numbers indicate better neutralization. Red fill indicates undetectable neutralization in our assay of >1,000 ng/mL.

Materials and Methods

Cloning for Plasmids Encoding Structural Proteins. pcDNA3.1 backbone plasmids were generated encoding N and M-IRES-E. Sequences for E, M, and N were PCR-amplified from codon-optimized plasmids, gifts from Nevan Krogan (UCSF, San Francisco, CA, USA; Addgene plasmid nos. 141385, 141386, and 141391). pcDNA3.1-SARS2-Spike was a gift from Fang Li (University of Minnesota, MN, USA; Addgene plasmid no. 145032). Site-directed mutagenesis (NEB) was used to remove the C9-tag and introduce the D614G mutation. Delta and Omicron structural protein were cloned ligating eBlocks (IDT) gene fragments following NEBuilder HiFi DNA (NEB E2621L) Assembly Reaction Protocol.

SC2-VLP Production. For a 24-well, plasmids CoV2-N (0.67), CoV2-M-IRES-E (0.33), CoV-2- Spike (0.006), and Luc-PS9 (1.0) at indicated mass ratios for a total of

1 μg of DNA were diluted in 50 μL Opti-MEM. Three micrograms of PEI (polyethyleneimine) was diluted in 50 μL Opti-MEM and added to plasmid dilution quickly to complex the DNA. Transfection mixture was incubated for 20 min at room temperature and then added dropwise to 293T cells in 0.5 mL of Dulbecco's modified Eagle's medium (DMEM) containing fetal bovine serum (FBS) and penicillin/streptomycin. Media was changed after 24 h of transfection, and at 48 h posttransfection VLP-containing supernatant was collected and filtered using a 0.45-μm syringe filter. For other culture sizes, the mass of DNA used was 1 μg for 24-well, 4 μg for 6-well, 20 μg for 10-cm plate, and 40 μg for 15-cm plate. Opti-MEM volumes were 100 μL, 400 μL, 1 mL, and 3 mL, respectively, and PEI was always used at 3:1 mass ratio.

Western Blot. For Western blots of lysates, media was removed and cells were rinsed with phosphate-buffered saline (PBS). Cells were then lysed for 20 min in N-PER lysis buffer containing Halt protease and phosphatase inhibitor mixture. For Western blots of ultracentrifuge-concentrated VLPs, 10 mL of VLP supernatant from a 10-cm plate was pelleted (28,000 rpm, 2 h, SW41 Ti, 1 mL 20% sucrose cushion), the supernatant was discarded, and VLPs were resuspended in 50 μL of PBS. Fifteen microliters of concentrated VLPs were used to Western blot. Laemmli loading buffer (1× final) and dithiothreitol (DTT, 40 mM final) were added to lysates or VLP solution and heated at 95 °C for 5 min to lyse VLPs and denature proteins. Samples were loaded on to 4 to 20% gradient gels (Bio-Rad) and transferred to a poly(vinylidene difluoride) membrane (Bio-Rad). Membrane was blocked in 3% BSA (N-staining) or 10% NFDM (all others) and stained with primary antibody: anti-N (Abcam ab273434, 1:500 dilution), anti-S (Abcam ab272504, 1:1,000), anti-GAPDH (Santa Cruz sc-365062, 1:1,000), or anti-p24 (Sigma, 1:2,000) for 2 h at room temperature. Blots were rinsed with TBS-T three times for 10 min each and stained with secondary antibody (Abcam ab205719, mouse, 1:5,000), and imaged using a Pierce chemiluminescence kit.

Northern Blot. VLPs collected from a 10-cm plate were concentrated by ultracentrifugation through a 20% sucrose cushion (28,000 rpm, 2 h, SW41 Ti). The supernatant was discarded and VLPs were resuspended in 50 μL of PBS. Twenty microliters of concentrated VLPs were used for Northern blotting. VLPs were lysed by adding 500 μL of TRIzol (Sigma) and RNA was extracted by phase separation, precipitated with isopropanol with GlycoBlue, and washed with 75% ethanol. RNA was resuspended in 30 μL of water, added to 30 μL 2× RNA Loading Dye (NEB) and denatured at 65 °C for 15 min then loaded onto a 1% agarose gel containing 1× MOPS and 4% formaldehyde. Samples were run at room temperature for 12 h at 20 V and transferred by capillary action to nylon membrane. The membrane was hybridized with a ^{32}P-labeled luciferase DNA probe (Prime-a-Gene Labeling System; Promega) and visualized using a phosphoscreen on a Typhoon imager (GE).

Quantification of Western and Northern Blots. Images were analyzed using Fiji. First, the background was subtracted using a 50-pixel-radius rolling ball and then total intensities were measured for each band. In the case of S protein, intensity of the bands corresponding to complete S and S2 were added together. Intensities of each band were first normalized based on the brightness of each blot and then normalized to the "All B.1" condition. Data were analyzed in GraphPad Prism using one-way ANOVA with repeated measures comparing each condition to the "All B.1" condition and using Dunnett's correction.

Luciferase Readout. In each well of a clear 96-well plate 50 μL of SC2-VLP–containing supernatant was added to 50 μL of cell suspension containing 50,000 receiver cells (293T ACE2/TMPRSS2). Cells were allowed to attach and take up VLPs overnight. The next day, supernatant was removed and cells were lysed in 20 μL passive lysis buffer (Promega) for 15 min at room temperature with gentle rocking. Lysates were transferred to an opaque white 96-well plate and 30 μL of reconstituted luciferase assay buffer was added and mixed with each lysate. Luminescence was measured immediately after mixing using a Tecan plate reader with no attenuation and a luminescence integration time of 1 s.

Cell Lines. Cells were maintained in a humidified incubator at 37 °C in 5% CO_2 in the indicated media and passaged every 3 to 4 d. The 293T cells were obtained from ATCC and maintained in DMEM with 10% FBS and 1% penicillin/streptomycin. The 293T cells stably coexpressing ACE2 and TMPRSS2 were generated through sequential transduction of 293T cells with TMPRSS2-encoding (generated using Addgene plasmid no. 170390, a gift from Nir Hacohen, Broad Institute, Cambridge, MA, USA) and ACE2-encoding (generated using Addgene plasmid no. 154981, a gift from Sonja Best, Rocky Mountain Labs, Hamilton, MT, USA) lentiviruses and selection with hygromycin (250 μg/mL) and blasticidin (10 μg/mL) for 10 d, respectively. ACE2 and TMPRSS2 expression was verified by Western blot. Vero stably coexpressing human ACE2 and TMPRSS2 cells (gifted from A. Creanga and B. Graham, NIH, Bethesda, MD) were maintained at 37 °C and 5% CO_2 in DMEM (Gibco) supplemented with 10% fetal calf serum, 100 ug/mL penicillin and streptomycin (Gibco), and 10 μg/mL of puromycin (Gibco).

VLP Neutralization Assay. Each heat-inactivated serum sample was serially diluted from 1:20 to 1:20,480 dilution in complete DMEM media prior to incubation (1 h at 37 °C) with 40 μL VLP with total volume of 50 μL, then plated onto receiver cells (50,000 293T ACE2-TMPRSS2 cells). Twenty-four hours later luciferase readout was taken. Neutralization (NT50) was estimated by interpolating the dilution of serum at which 50% infectivity was reduced.

Serum Samples. Serum samples from individuals not exposed to SARS-CoV-2 (pre-COVID, control), exposed to SARS-CoV-2 (post-COVID), and those vaccinated with either two doses of elasomeran (Moderna), two doses of tozinameran (Pfizer/BioNTech) vaccine, or one dose of Johnson & Johnson vaccine were collected through a clinical trial led by Curative (*SI Appendix*, Table S5). Post-COVID samples reflect nonvaccinated participant samples that were collected within 4 to 6 wk of the original positive test and were negative by PCR at the time of serum collection. Serum from vaccinated participants was collected 4 to 6 wk postvaccination following final dose. The clinical trial protocol was approved by Advarra under Pro00054108 for a study designed to investigate immune escape by SARS-CoV-2 variants. The trial has been submitted to the clinicaltrials.gov registry (NCT05171803, Unique Protocol ID: PTL-2021-0007). Sample specimens were collected from adult individuals aged 18 to 50 y who either had been vaccinated for COVID-19 and/or had a history of COVID-19. Vulnerable populations were excluded from enrollment. Patients signed consent forms held by Curative. Participants were enrolled from individuals that tested with Curative in Los Angeles County and were sent an institutional review board–approved email enrollment script. Those who were interested were contacted by the Curative Clinical Trials research team (CITI trained) and those who consented to the study were scheduled for sample collection by a clinician who went to their residence. Participants underwent a standard venipuncture procedure. Briefly, licensed phlebotomists collected a maximum of 15 mL whole blood. Once collected, the sample was left at ambient temperature for 30 to 60 min to coagulate then was centrifuged at 2,200 to 2,500 rpm for 15 min at room temperature. Samples were then placed on ice until delivered to the laboratory site where the serum was aliquoted to appropriate volumes for storage at −80 °C until use. A quantitative SARS-CoV-2 IgG ELISA was performed on serum specimens (EuroImmun, Anti-SARS-CoV-2 ELISA [IgG], 2606-9621G, NJ). To quantify SARS-CoV-2 IgG antibodies, an S1-specific monoclonal IgG antibody with no known cross-reactivity to the S2 domain of the spike protein was used as a reference antibody. A standard curve was developed using a monoclonal IgG antibody targeting the S1 antigen of SARS-CoV-2 at different concentrations with a polynomial regression curve-fitting model. The standard curve was used to calculate the sample IgG antibody concentration. Serum samples were heat-inactivated at 56 °C for 30 min prior to use in VLP assays. Pre-COVID sera was pooled into one sample.

SARS-CoV-2 Culture. SARS-CoV-2/human/USA/USA-WA1/2020 (WA1) (BEI NR-52281), B.1.617.2 (BEI NR-55611), and B.1.1.529 (California Department of Health) were used for serum virus neutralization. The virus infection experiments were performed in a Biosafety Level 3 laboratory. Working stocks of SARS-CoV-2 were made in Vero-TMPRSS2 cells and were stored at −80 °C until used.

Virus Neutralization Assay. Serum dilutions (50 μL) of 1:5, 1:15, 1:45, 1:135, 1:405, and 1:1,215 were prepared in serum-free DMEM. The dilutions were separately added with 50 plaque-forming units (50 μL) of SARS-CoV-2 WA1, B.1.617.2, or B.1.1.529. The mixture was mixed gently and incubated at 37 °C for 30 min, followed by a plaque assay.

Plaque Assays. Vero-TMPRSS2 were seeded and incubated overnight. The cells were inoculated with the neutralized inoculum in serum-free DMEM. After the 1-h absorption period, the media in the wells was overlaid with 2.5% Avicel (Dupont, RC-591). After 72 h, the overlay was removed, the cells were fixed in 10% formalin for 1 h and stained with crystal violet for visualization of plaque-forming units.

Data Availability. All study data are included in the article and/or *SI Appendix*.

ACKNOWLEDGMENTS. We thank members of the J.A.D. and M.O. laboratories for helpful discussions. This project was funded by a grant from the National Institutes of Health (R21AI59666) and by support from the Howard Hughes Medical Institute and the Gladstone Institutes. A.M.S. acknowledges the support of the Natural Sciences and Engineering Research Council of Canada (NSERC PDF-533021-2019) and I.P.C. support from the NIH (F31 AI164671-01).

Author affiliations: [a]Gladstone Institutes, San Francisco, CA 94158; [b]Innovative Genomics Institute, University of California, Berkeley, CA 94720; [c]School of Medicine, Vanderbilt University, Nashville, TN 37232; [d]Curative Inc., San Dimas, CA, 91773; [e]Department of Medicine, University of California, Los Angeles, CA 90095; [f]Department of Medicine, University of California, San Francisco, CA 94143; [g]Chan Zuckerberg Biohub, San Francisco, CA 94158; [h]Department of Molecular and Cell Biology, University of California, Berkeley, CA 94720; [i]HHMI, University of California, Berkeley, CA 94720; [j]Department of Chemistry, University of California, Berkeley, CA 94720; [k]Molecular Biophysics and Integrated Bioimaging Division, Lawrence Berkeley National Laboratory, Berkeley, CA 94720; and [l]California Institute for Quantitative Biosciences (QB3), University of California, Berkeley, CA 94720

Author contributions: A.M.S., G.R.K., M.O., and J.A.D. designed research; A.M.S., A.C., T.Y.T., I.P.C., M.M.K., B.S., P.-Y.C., R.S., and T.T. performed research; I.S., B.M., N.K., V.H., M.S., L.L., M.B., F.T., and L.S. contributed new reagents/analytic tools; A.M.S. analyzed data; and A.M.S., L.S., M.O., and J.A.D. wrote the paper.

Competing interest statement: A.M.S. and J.A.D. are inventors on a patent application filed by the Gladstone Institutes and the University of California that covers the method and composition of SARS-CoV-2 VLP preparations for RNA transduction and expression in cells. J.A.D. is also a cofounder of Caribou Biosciences, Editas Medicine, Scribe Therapeutics, Intellia Therapeutics, and Mammoth Biosciences. J.A.D. is a scientific advisory board member of Vertex, Caribou Biosciences, Intellia Therapeutics, Scribe Therapeutics, Mammoth Biosciences, Algen Biotechnologies, Felix Biosciences, The Column Group, and Inari. J.A.D. is Chief Science Advisor to Sixth Street, a Director at Johnson & Johnson, Altos and Tempus, and has research projects sponsored by Biogen, Pfizer, AppleTree Partners, and Roche.

1. K. H. D. Crawford *et al.*, Protocol and reagents for pseudotyping lentiviral particles with SARS-CoV-2 spike protein for neutralization assays. *Viruses* **12**, E513 (2020).
2. J. A. Plante *et al.*, Spike mutation D614G alters SARS-CoV-2 fitness. *Nature* **592**, 116–121 (2021).
3. A. M. Syed *et al.*, Rapid assessment of SARS-CoV-2-evolved variants using virus-like particles. *Science* **374**, 1626–1632 (2021).
4. A. J. Greaney *et al.*, Complete mapping of mutations to the SARS-CoV-2 spike receptor-binding domain that escape antibody recognition. *Cell Host Microbe* **29**, 44–57.e9 (2021).
5. S. Cele *et al.*, SARS-CoV-2 Omicron has extensive but incomplete escape of Pfizer BNT162b2 elicited neutralization and requires ACE2 for infection. medRxiv [Preprint] (2021). https://www.medrxiv.org/content/10.1101/2021.12.08.21267417v3 (Accessed 27 June 2022).
6. L. Lu *et al.*, Neutralization of SARS-CoV-2 Omicron variant by sera from BNT162b2 or Coronavac vaccine recipients. *Clin. Infect. Dis.*, 10.1093/cid/ciab1041 (2021).